Nanoflares and Heating of the Solar Corona

U. Narain* & K. Pandey
Astrophysics Research Group, Meerut College, Meerut 250 001, India.
*e-mail: uditnarain@yahoo.co.in

Abstract. Coronal heating by nanoflares is presented by using observational, analytical, numerical simulation and statistical results. Numerical simulations show the formation of numerous current sheets if the magnetic field is sheared and bipoles have unequal pole strengths. This fact supports the generation of nanoflares and heating by them. The occurrence frequency of transients such as flares, nano/microflares, on the Sun exhibits a power-law distribution with exponent α varying between 1.4 and 3.3. For nanoflares heating α must be greater than 2. It is likely that the nanoflare heating can be reproduced by dissipating Alfvén waves. Only observations from future space missions such as Solar-B, to be launched in 2006, can shed further light on whether Alfvén waves or nanoflares, heat the solar corona.

Key words. Sun: stars—magnetic reconnection: coronal heating—nanoflares.

1. Introduction

It is well-known that the solar corona is a few hundred times hotter than the underlying atmospheric regions (chromosphere and photosphere). Two heating agents involving magnetic fields, namely MHD waves and transients (such as flares, nano- and microflares) are the most favoured ones (see, e.g., Narain & Ulmschneider 1996; Pandey & Narain 2001; Dwivedi 2002, 2003; Walsh & Ireland 2003; Aschwanden 2004 and references therein). In this article heating by nanoflares (Parker 1988, 1991) is briefly described and discussed.

Section 2 estimates the energy of a nanoflare as a result of a single magnetic reconnection. In section 3, we exhibit the power-law distribution of transients. Section 4 contains a brief description of observational and theoretical efforts made in this direction. The last section contains our conclusions.

Throughout the cgs system of units has been used.

2. Energy of a nanoflare

It is thought that when two oppositely directed magnetic fields come closer to form a current sheet, the current density of contained plasma increases considerably so that a small resistivity is quite sufficient to convert magnetic energy to thermal energy via magnetic reconnection and resulting turbulence. This is shown in Fig. 1.
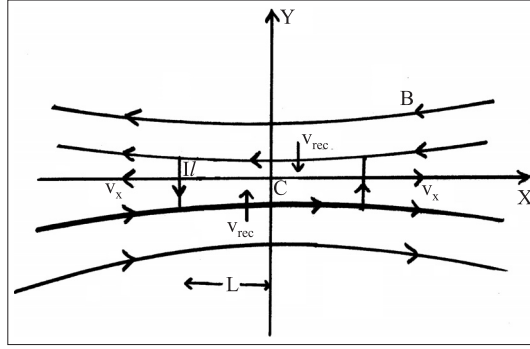
Figure 1.

The current sheet has length $2L$ and breadth $2l$. The magnetic field component B_X reverses direction along the line $y = 0$, assuming field geometry to be independent of coordinate z (directed out of paper) following Tandberg-Hanssen and Emslie (1988), the current density in the current sheet is given by:

$$j = \frac{cB_X}{4\pi l},\tag{1}$$

where j is the current density and c is the speed of light in vacuum. Equation (1) shows that as l becomes smaller j becomes larger. The merging of oppositely directed field lines, which decreases l, is limited by the gas pressure p between the oppositely directed fields. Since the field and plasma are frozen together, the following equation is satisfied:

$$p = \frac{B_X^2}{8\pi}.\tag{2}$$

Outside the region $|x| > L$, the gas pressure is much smaller than inside the current sheet, $|x| < L$, so that the fluid is ejected along the field lines (x-direction, Fig. 1), reducing the built-up pressure.

In the steady state the momentum equation for the plasma, ejected along the field lines is

$$\rho v_x \left(\frac{\partial v_x}{\partial x} \right) = \frac{-\partial p}{\partial x},\tag{3}$$

where ρ is the matter density of fluid. Assuming fluid to be incompressible, equation (3) may be integrated from $x = 0$ to $x = L$, corresponding to $p = p_i$ and $p = p_0$, to get

$$0.5\rho v_x^2(L) = p_i - p_0.\tag{4}$$

By symmetry $v_x(x = 0) = 0$ and the pressure difference $p_i - p_0$ is due to the magnetic field pressure $B_x^2/8\pi$ within the region $|x| \leq L$ so that equation (4) gives

$$v_X(L) = \frac{B_X}{(4\pi\rho)^{0.5}} = v_A,\tag{5}$$

where v_A is the Alfvén speed within the reconnecting region. The reconnection velocity $v_{rec}(= dl/dt)$ gives the rate at which the magnetic field lines are swept into the reconnecting volume, V.

The continuity equation, under incompressibility conditions, demands that the outward flow of matter along the x-axis must be balanced by an inflow in the y-direction so that

$$v_{rec}L = v_A l. \tag{6}$$

Further, in the steady state, the ohmic dissipation, ηj^2, of energy in the reconnecting region must be just sufficient to balance the influx of magnetic energy in that region, i.e.,

$$\iiint_V \eta J^2 dV = \iint_S \left(\frac{B_x^2}{8\pi}\right) v_x dS$$

which, in view of equation (6), Fig. 1 and per unit length in the z-direction gives

$$j^2 = \frac{B_x^2 v_{rec}}{8\pi \eta l}, \tag{7}$$

where η is the resistivity of the fluid in the current sheet. Comparing equations (1) and (7) leads to

$$v_{rec}^2 = \frac{\eta c^2 v_A}{2\pi L} \tag{8}$$

and

$$l^2 = \frac{\eta c^2 L}{2\pi v_A}. \tag{9}$$

The longitudinal magnetic Reynolds number, R_{ml}, provides the effect of diffusion over dissipation and is defined by

$$R_{ml} = \frac{\left|\vec{\nabla}x(\vec{v}x\vec{B})\right|}{\left|\eta c^2 \nabla^2 \vec{B}/4\pi\right|} \approx \frac{8\pi L v_A}{\eta c^2}. \tag{10}$$

Equations (8), (9) and (10) now give

$$v_{rec} = \frac{2v_A}{R_{ml}^{0.5}} \tag{11}$$

and

$$l = \frac{2L}{R_{ml}^{0.5}}. \tag{12}$$

Defining Alfvén crossing time, t_A, and reconnection time, t_R, by

$$t_A = \frac{l}{v_A} \tag{13}$$

and

$$t_R = \frac{l}{v_{\text{rec}}}, \tag{14}$$

equations (11) and (12) give

$$t_R = 0.5 t_A R_{ml}^{0.5}. \tag{15}$$

The rate of energy release in the current sheet may be obtained from the following:

$$\frac{dE}{dt} = \frac{B^2 V}{8\pi t_R}, \tag{16}$$

where B is the magnetic field strength before reconnection (dissipation). The resistivity, η, for the solar corona is determined using the following expression (Spitzer 1962):

$$\eta = 1.5 \times 10^{-7} T^{-1.5}. \tag{17}$$

For a rough estimate, we take $L = 10^9$ cm, $B = 300$ G, electron/proton number density $n = 10^{10}$ cm^{-3} and $T = 2$ MK. This gives:

$$v_A = 6 \times 10^8 \text{ cm s}^{-1}, \quad \eta = 5 \times 10^{-17} \text{ s}, \quad R_{ml} = 10^{14}, \quad l = 200 \text{ cm},$$

$$t_A = 3 \times 10^{-5} \text{ s} \quad \text{and} \quad t_R = 2 \text{ s}.$$

Taking $V = L^2 l = 2 \times 10^{20}$ cm^2, equation (16) together with above values gives:

$$\frac{dE}{dt} = 4 \times 10^{23} \text{ erg s}^{-1}. \tag{18}$$

Thus the energy released from the magnetic reconnection in a single current sheet equals that of a nanoflare.

3. Power-law distribution

Parker (1988) proposed that the energy dissipation of the stressed magnetic structure takes place in a large number of small events, which he termed nanoflares. The superposition of a large number of such events may give the global appearance of a spatially homogenous and stationary heating process. The spiky (both in space and time) heating of nanoflares may be related to global heating as follows:

If E_t be the total heating rate contributed by all the events in the energy range $E_{\min}$, $E_{\max}$ then

$$E_t = \int_{E_{\min}}^{E_{\max}} P(E) E \, dE, \tag{19}$$

where $P(E)$ is the number of events per unit energy range and time. This occurrence rate displays the following power-law behaviour (Pandey & Narain 2001 and references therein):

$$P(E) = A E^{-\alpha}, \tag{20}$$

where A and α are some constants. On combining equations (19) and (20) we get:

$$E_t = \frac{A(E_{\max}^{2-\alpha} - E_{\min}^{2-\alpha})}{(2-\alpha)}. \tag{21}$$

3.1 *Case I: $\alpha < 2$*

Since $E_{\max} \gg E_{\min}$, therefore the second term in equation (21) may be dropped to get

$$E_t^I = \frac{A E_{\max}^{2-\alpha}}{(2-\alpha)}. \qquad (22)$$

That is, the heating will be dominated by high energy events, namely large and intermediate energy flares.

3.2 *Case II: $\alpha > 2$*

In this case the first term in equation (21) may be dropped to get

$$E_t^{II} = \frac{A E_{\min}^{2-\alpha}}{(\alpha-2)}. \qquad (23)$$

That is, the heating is dominated by the low-energy events, namely micro- and nano-flares.

4. Results and discussion

It seems quite interesting to start with Georgoulis and Vlahos (1996) who developed a cellular automation self-organised critical (SOC) model for transients in which an explosion affects its neighbourhood by lowering the instability criteria and igniting secondary bursts triggered by an initial instability in an avalanche type manner. In the resulting frequency distributions (cf. equation (20)) they obtain two distinct power laws. The weaker events have shorter and steeper power law with exponent $\alpha \approx 3.26$ whereas the large and intermediate events have $\alpha \approx 1.73$. Also the weaker events are responsible for almost 90% of the total magnetic energy released and thus support coronal heating by nanoflares. This model has been further improved by Georgoulis *et al.* (2001).

In order to know whether heating is dominated by low or high energy events we compile the values of power-law exponent, α in Table 1 for the solar corona. It contains both, the theoretically and observationally deduced values.

An examination of Table 1 shows that both types of cases, i.e., $\alpha < 2$ and $\alpha > 2$ exist. No clear picture emerges. There is some controversy over the method of determination of values of α (see, e.g., McIntosh & Charbonneau 2001; Aschwanden & Charbonneau 2002a).

Karpen *et al.* (1996) and Antiochos *et al.* (2002) have performed numerical simulations of the interaction between two bipoles through magnetic reconnection in the lower solar atmosphere. Here the magnetic field is sheared asymmetrically and the bioples have markedly unequal field strengths. They arrive at the most exciting and potentially far-reaching discovery that the random nature of reconnection process creates a distribution of current sheets throughout the region occupied by reconnected field lines. Reconnection between the larger and smaller flux systems leads to long-lived current sheets that decay slowly and yield the observed X-ray structures.

Table 1. The power-law exponent, α.

Object	Phenomenon/instrumentation	Value	References
Sun	Type I radio burst	3	Mercier & Trottet (1997)
Sun	Iron lines/EIT (SOHO)	2.3–2.6	Krucker & Benz (1998)
XBP (Sun)	X-ray/Yohkoh	1.7 ± 0.4	Shimojo & Shibata (1999)
Quiet Sun	171 Å, 195 Å/TRACE	1.83 ± 0.07	Aschwanden *et al.* (2000)
Quiet Sun	EUV/CDS (SOHO)	2.5 (Cell) 1.7 (Network)	Harra *et al.* (2000)
Sun	CIII 977 Å, NIV 765 Å, OVI 1032 Å, NeVIII/SUMER	2.9 ± 0.1	Winebarger *et al.* (2002)
Solar coronal loop	2d-MHD/simulation	1.5	Dmitruk & Gomez (1997, 1999)
Solar coronal loop	1d-MHD compressible/ simulation	1.57 (large events) ≥ 1.81 (nanofalres)	Galtier (1999)
Solar corona	Flarelike processes 0.7–1.1 MK 1.0–1.5 MK 2.0–4.0 MK Hard X-rays	1.86 ± 0.07 1.81 ± 0.10 1.57 ± 0.15 1.4–1.6	Aschwanden & Parnell (2002b)
Solar corona	SOC Model/weak events large and intermediate events	3.26 1.73	Georgoulis & Vlahos (1996)

Another interesting and important result comes from Moriyasu *et al.* (2004) who examine the creation of hot corona in an initially cool loop as a result of nonlinear Alfvén waves. Here the dissipation takes place via mode- coupling with slow- and fast-mode waves which is balanced by conduction and radiative cooling. Their numerical simulations reveal that the resulting corona is very dynamic and full of shocks so that the temporal variation of the X-ray and EUV intensities shows many nanoflare-type events, quite similar to what is actually observed. In fact, the occurrence frequency of X-ray and EUV nanoflares as a function of their peak intensity is a power-law distribution with an index ~ 1.7 for X-ray and ~ 1.39 for EUV. Quite obviously, the actual observed time variation of the X-ray and EUV fluxes in the corona and in the chromosphere, may not be evidence of small scale magnetic reconnections but could actually be due to Alfvén waves.

In another landmark work Cargill and Klimchuk (2004) investigate the radiative signatures of the nanoflare-heated corona and speculate that if an observed coronal loop contains many small strands then continual heating and cooling of strands would lead to a corona having a multi-thermal structure. The cyclical heating–cooling makes the loops have lower and higher densities at high and low temperatures, respectively. The respective underdensity and overdensity at high and low temperatures have been reported in the analyses of coronal data by Winebarger *et al.* (2003).

5. Conclusions

The matter presented in the foregoing sections leads us to arrive at the following conclusions:

- The stressing models (including nanoflare scenario) involving slow footpoint motions of loops appear to be in a better position to explain coronal heating.
- Frequency distribution of nanoflare energies is a power-law with exponent α which must be greater than 2. The value of this exponent is still ambiguous and controversial.
- The actual observed time variation of the X-ray and EUV fluxes in the solar atmosphere may not be an evidence of small-scale magnetic reconnections (nanoflares) but could well be due to dissipation of Alfvén waves.
- The signatures of coronal heating processes should be searched in the transition region and lower corona because these regions have relatively smaller time scales.
- Only observations are capable of deciding whether the corona is primarily heated by nanoflare-like events or by Alfvén waves. For example, the Extreme Ultraviolet Imaging Spectrometer on Solar-B Satellite (to be launched in 2006) is capable of deciding whether the nanoflare events are actually MHD shocks due to Alfvén waves or not?

References

Antiochos, S. K., Karpen, J. T., De Vore, C. R. 2002, *ApJ*, **575**, 570.
Aschwanden, M. 2004, Physics of the Solar Corona, An Introduction, Springer, Praxis Publication.
Aschwanden, M. J., Nightingale, R. W., Tarbell, T. D., Wolfson, C. J. 2000, *ApJ*, **535**, 1027.
Aschwanden, M. J., Charbonneau, P. 2002a, *ApJ*, **566**, L59.
Aschwanden, M. J., Parnell, C. E. 2002b, *ApJ*, **572**, 1048.
Cargill, P. J., Klimchuk, J. A. 2004, *ApJ*, **605**, 911.
Dmitruk, P., Gomez, D. O. 1997, *ApJ*, **484**, L83.
Dmitruk, P., Gomez, D. O. 1999, *ApJ*, **527**, L63.
Dwivedi, B. N. 2002, *BASI*, **30**, 549.
Dwivedi, B. N. 2003, In: *Lectures on Solar Physics* (ed.) H. M. Antia *et al.* Springer, Berlin, p. 281.
Galtier, S. 1999, *ApJ*, **521**, 483.
Georgoulis, M. K., Vlahos, L. 1996, *ApJ*, **469**, L135.
Georogoulis, M. K., Vilmer, N., Crossby, N. B. 2001, *A&A*, **367**, 326.
Harra, L. K., Gallagher, P. T., Phillips, K. J. H. 2000, *A&A*, **362**, 371.
Karpen, J. T., Antiochos, S. K., De Vore, C. R. 1996, *ApJ*, **460**, L73.
Krucker, S., Benz, A. O. 1998, *ApJ*, **501**, L213.
McIntosh, S. W., Charbonneau, P. 2001, *ApJ*, **563**, L165.

Mercier, C., Trottet, G. 1997, *ApJ*, **474**, L65.

Moriyasu, S., Kudoh, T., Yokoyama, T., Shibata, K. 2004, *ApJ*, **601**, L107.

Narain, U., Ulmscheider, P. 1996, *Space Sci. Rev.*, **75**, 453.

Pandey, K., Narain, U. 2001, *BASI*, **29**, 231.

Parker, E. N. 1988, *ApJ*, **330**, 474.

Parker, E. N. 1991, In: Mechanisms of Chromospheric & Coronal Heating (eds) P. Ulmschneider, E. R. Priest, R. Rosner, Springer, Berlin, p. 615.

Shimojo, M., Shibata, K. 1999, *ApJ*, **516**, 934.

Spitzer, L. 1962, Physics of Fully Ionized Gases, John Wiley, New York.

Tandberg-Hanssen, E., Emslie, A. G. 1988, The Physics of Solar Flares, Cambridge Univ. Press, Cambridge.

Walsh, R. W., Ireland, J. 2003, *A&A Rev.*, **12**, 1.

Winebarger, A. R., Emslie, A. G., Mariska, J. T., Warren, H. P. 2002, *ApJ*, **565**, 1298.

Winebarger, A. R., Warren, H. P., Mariska, J. T. 2003, *ApJ*, **587**, 439.